Rare Metal Materials and Engineering
Volume 54, Issue 1, January 2025
Available online at www.rmme.ac.cn

Science Press

Cite this article as: Zhang Zhe, Liu Hui, Lin Manfeng, et al. Physical Antibacterial Surface Modifications on Titanium-Based Implant Materials[J]. Rare Metal Materials and Engineering, 2025, 54(01): 84-93. DOI: 10.12442/j.issn.1002-185X.20240527.

REVIEW

Physical Antibacterial Surface Modifications on Titanium-Based Implant Materials

Zhang Zhe, Liu Hui, Lin Manfeng, Cai Zongyuan, Zhao Dapeng

College of Biology, Hunan University, Changsha 410082, China

Abstract: Infections associated with titanium (Ti)-based implants present significant challenges in clinical treatments, especially when biofilms already form on the implant surface. Many antimicrobial agents, including antibiotics, metallic nanoparticles and antimicrobial peptides, have been extensively used to deal with Ti implant infections. However, these chemical approaches suffer from potential toxicity, antibiotic resistance and poor long-term antibacterial performance. Hence, physical antibacterial surfaces on Ti-based implants have attracted increasing attention. The antibacterial behavior of different surfaces on Ti-based biomaterials against various bacteria only by physical properties of the implants themselves (e.g., nanotopography) or exogenous physical stimulus (e.g., photocatalysis) was reviewed, as well as parameters influencing the physical antibacterial processes, such as size, shape and density of the surface nanotextures, and bacterial growth phases. Besides, mechanisms of different fabrication techniques for the physical antibacterial surfaces on Ti-based biomaterials were also summarized.

Key words: physical antibacterial behavior; surface modification; titanium alloy; implant material

Titanium (Ti)-based alloys are widely used in orthopedic and dental fields due to their excellent corrosion resistance, superior mechanical properties, and good biocompatibility[1–4]. However, Ti alloys are susceptible to bacterial infections[5–6]. Currently, the global infection risk for orthopedic surgeries is about 2% – 5%[7]. Bacteria around implants can rapidly colonize and form biofilms within hours of post-implantation, leading to infections[8–9]. This can adversely affect the adhesion of osteoblast-related cells to the surface, ultimately resulting in poor osseointegration[10–11]. Worse still, severe infection after implantation leads to the failure of the implant surgery, necessitating multiple additional operations[12].

To deal with postoperative infections, clinical treatments for patients often rely on multiple debridement surgeries and systemic antibiotic administration. However, once a mature biofilm forms on any implant surface, it becomes challenging to eradicate bacteria despite antibiotic treatments and repeated surgical washouts[13]. This leads to the emergence and spread of multidrug-resistant bacteria[14], making it difficult to fully recover, and imposes physical suffering and economic burdens on the patients[15]. Therefore, there is a need for Ti implants capable of repelling or eliminating bacteria in the early stages of implantation and promoting osseointegration in the later stages to solve this issue[16–18].

Many researchers focus on the application of chemical antibacterial coatings onto the surface of Ti-based implants. These coatings can actively kill bacteria or passively prevent their adhesion. Surface-modified implants based on antibacterial coatings can inhibit bacterial infection by releasing antimicrobial agents, such as antibiotics, Ag ions, Cu ions, antimicrobial peptides and other antimicrobial macromolecules[13]. However, the potential toxicity of these antimicrobial agents cannot be ignored[19], and the stability of these coatings in practical applications has yet to be verified. The abovementioned limits of chemical antibacterial surface treatments lead to the development of better antibacterial modifications on Ti-based implant surfaces. Recently, physical antibacterial surfaces have drawn increasing attention, because killing bacteria through physical mechanisms is much safer and more sustainable[20].

1 Natural Physical Antibacterial Surfaces

Physical antibacterial surfaces are ubiquitous in nature,

Received date: August 15, 2024
Foundation item: National Natural Science Foundation of China (52171114)
Corresponding author: Zhao Dapeng, Ph. D., Associate Professor, College of Biology, Hunan University, Changsha 410082, P. R. China, Tel: 0086-731-88822606, E-mail: dpzhao@hnu.edu.cn

with a multitude of creatures exhibiting these surfaces to protect themselves against pathogenic bacteria[21]. Early studies attributed these antibacterial effects to the inhibition of bacterial adhesion due to hydrophilic or hydrophobic properties[22–24]. However, recent research has discovered that these antibacterial effects are achieved through the interaction between bacteria and the nanostructures on natural antibacterial surfaces, known as the contact-killing mechanism[25].

Ma et al[24] found that, whether under dry or fully submerged conditions, the dense nanostructured epidermal wax crystals on the epidermal cells of taro leaves, as shown in Fig. 1a–1b, could resist the adhesion of *P. aeruginosa* cells or particles. It suggests that nanostructures with appropriate configurations may reduce bacterial contamination in underwater applications.

Ivanova et al[26] reported the bactericidal effects of the naturally bactericidal surface of cicada wings on *P. aeruginosa*. The nanopillars on the cicada wings, as shown in Fig. 1c–1d, can kill most bacterial cells within 5 min of contact. The time required for the nanopillars to rupture the bacterial cell wall is only approximately 3 min. It has been proposed that there is a 20 min adhesion/killing cycle, during which the cicada wing surface becomes saturated with bacteria. Once the bacteria are killed and either fragmented or sunk into the nanopillars, new bacteria can attach to the surface.

These unique bactericidal properties have garnered significant research interest due to their ability to prevent biofilm formation and infections on implant devices solely by the physical contact between the implant surface and bacteria. This antibiotic-free approach effectively kills antibiotic-resistant bacteria and mitigates the issue of resistant strain diversity caused by the misuse of drugs[27]. Additionally, many chemical antibacterial surfaces are only effective in the aqueous solutions, and potentially show reduced efficacy in killing bacteria that contact implants in the air when no liquid medium is present.

Some studies explore alternative physical methods to kill bacteria through the contact-killing mechanism rather than chemical means[28–30]. Models of contact-killing processes include the biophysical model, the elastic mechanics model, and the quantitative thermodynamics model[31]. Pogodin et al[32] demonstrated a biophysical model of the interaction between bacterial cells and the nanopatterned cicada wing surface, and found that the stiffness of bacterial cells was a crucial factor influencing the bactericidal effect of nanostructures. Xue et al[33] constructed an elastic mechanics model and concluded that the antibacterial performance of nanopillars was enhanced when the tip radius of the nanopillars was smaller and the spacing between pillars increased. Li et al[34] proposed a quantitative thermodynamic model, and the theoretical results indicated that the balance between the adhesion energy and deformation energy of the bacterial cell membrane played a decisive role in bacterial adhesion to nanostructures. These studies reveal the antibacterial mechanisms of natural physical surfaces. Multiple factors influence the antibacterial efficacy of natural surfaces, including microbial adhesion forces to the nanostructures[25, 35], the rigidity of bacterial cells[32], and the topographical morphology of the nanostructures[33].

2 Nanostructured Physical Antibacterial Surfaces on Ti-based Implant Materials

2.1 Amorphous nanomorphology

Inspired by the antimicrobial properties of natural surface

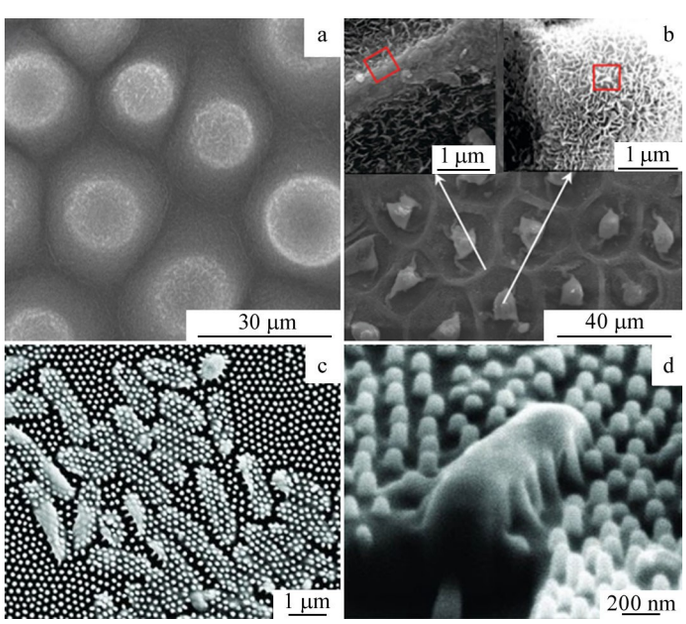

Fig.1 Scanning electron microscope (SEM) images of taro leaves after liquid substitution (a), air drying and sputter coating (b)[24]; *P. aeruginosa* cells on the surface of the cicada wing, with cell membranes visibly disrupted by the nanopillar structures (c); *P. aeruginosa* cells sinking between the nanopillars on the cicada wing surface (d)[26]

structures, researchers have explored the effects of surface morphology on bacterial behavior by simply altering the roughness[36] and crystalline phase[37–38] of Ti implants since 2006. Preliminary studies revealed that some nanoscale rough structures can significantly inhibit bacterial growth and proliferation. For example, some studies developed nanostructured antibacterial surfaces, covered with irregular nanowires as shown in Fig. 2[39–41]. These nanostructured surfaces not only demonstrate significant bactericidal capabilities but also show potential in long-term inhibition of biofilm formation by effectively disrupting the growth and maturation of biofilms over extended periods. Moreover, similar experiments conducted on three-dimensional substrates also confirm the effectiveness of these nanostructures in various dimensions and complex environments[42]. These findings suggest that such surface structures can substantially reduce the incidence of implant-associated infections in practical applications, providing new insights and directions for the design and optimization of medical implants[42].

2.2 Titania nanopillars

Due to technical limitations, the detailed mechanisms by which irregular nanoscale structures promote bone formation remain unclear[43], and there is no consensus on the exact mechanisms leading to microbial cell death[31]. To elucidate these mechanisms and achieve intentional control of cellular activity using the surface structures of implants, standardized, controllable, and periodic nanoscale Ti surface structures were fabricated.

Techniques such as thermal oxidation[44], reactive ion etching (RIE)[45], and electron beam lithography[46] can create well-ordered nanopillar structures on titanium surfaces. Nanopillars fabricated via RIE have demonstrated high bactericidal performance. Within 4 h of contact with the nanopillars, 95%±5% of *E. coli*, 98%±2% of *P. aeruginosa*, 92%±5% of *M. smegmatis*, and 22%±8% of adhered *S. aureus* cells were killed. After 24 h of cell adhesion, the bactericidal efficiency against *S. aureus* increased to 76%±4%[45].

Current research on the interactions between bacteria and nanopillars indicates that the primary antibacterial effect is attributed to nanomechanical stress induced by the contact of bacterial cells with nanostructured surfaces. Specifically, upon contact with nanopillars, the bacterial membrane experiences stretching and damage due to the nanomechanical stress exerted by the interaction with the nanopillars[33,47]. Fig. 3a–3f illustrate the deformation of the bacterial cell membrane upon contact with the nanopillars. Statistical results indicated that the envelope of *S. aureus* was largely unaffected by the nanopillars, with a low frequency of membrane deformation and penetration, observed in only 5% of cells. In contrast, the nanopillars caused significant deformation of the *E. coli* membrane. Indentations in contact with the nanopillar tips were observed in 26% of cells, and membrane penetration occurred in 19% of cells. For *K. pneumoniae*, the nanopillars induced membrane deformation in 11% of cells and penetrated the bacterial envelope in 8% of cells[31]. The weaker effect on the bacterial membranes of Gram-positive bacteria is attributed to the thickness of the peptidoglycan layer in their cell walls, which is 4 – 8 times thicker than that of Gram-negative bacteria[48]. This increased thickness provides Gram-positive bacteria with a greater resistance to membrane deformation due to mechanical stress.

The topological morphology (e. g., density, spacing, slope and aspect ratio) and adhesion force of biomimetic nanopillar structures significantly influence their interactions with bacteria. Analytical models suggest that upon contact with nanopillar surfaces, the adhesion forces exerted on the bacterial membrane induce stretching, ultimately leading to rupture and cell death. The tip radius of surface nanotextures is crucial, as it represents the initial contact point between bacteria and the implant. Smaller tips enhance bactericidal efficacy by exerting pressure on the bacterial membrane[49]. Zahir et al[50] demonstrated bactericidal activity against *S. aureus* and *P. aeruginosa* by constructing rod-shaped nanopillars with spherical caps, as shown in Fig. 3c – 3f. According to the simulations by quantitative thermodynamic model, as shown in Fig. 3g – 3h[34], it can be found that tip radius ranging from 50 nm to 60 nm significantly enhances the bactericidal effect, as this radius is sufficiently large to prevent the bacterial membrane from easily slipping off, yet small enough to exert significant pressure on the membrane, driving its deformation and rupture[51]. This suggests that

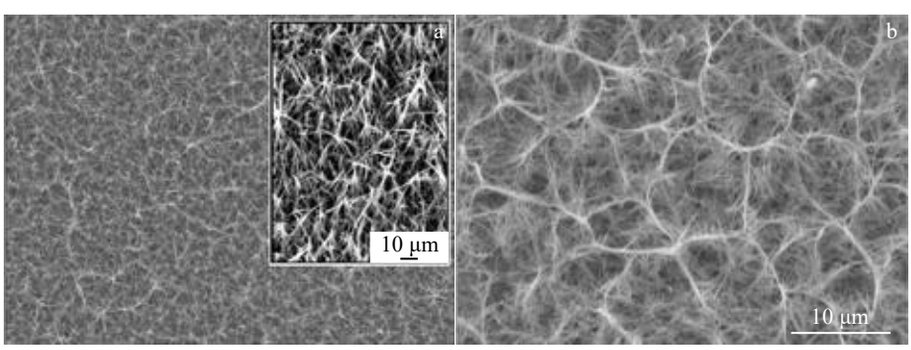

Fig.2 SEM images of brush (a) and niche (b) type patterns of amorphous titania nanowire arrays (30° tilted view of the brush type showing sharp nanowire tips)[41]

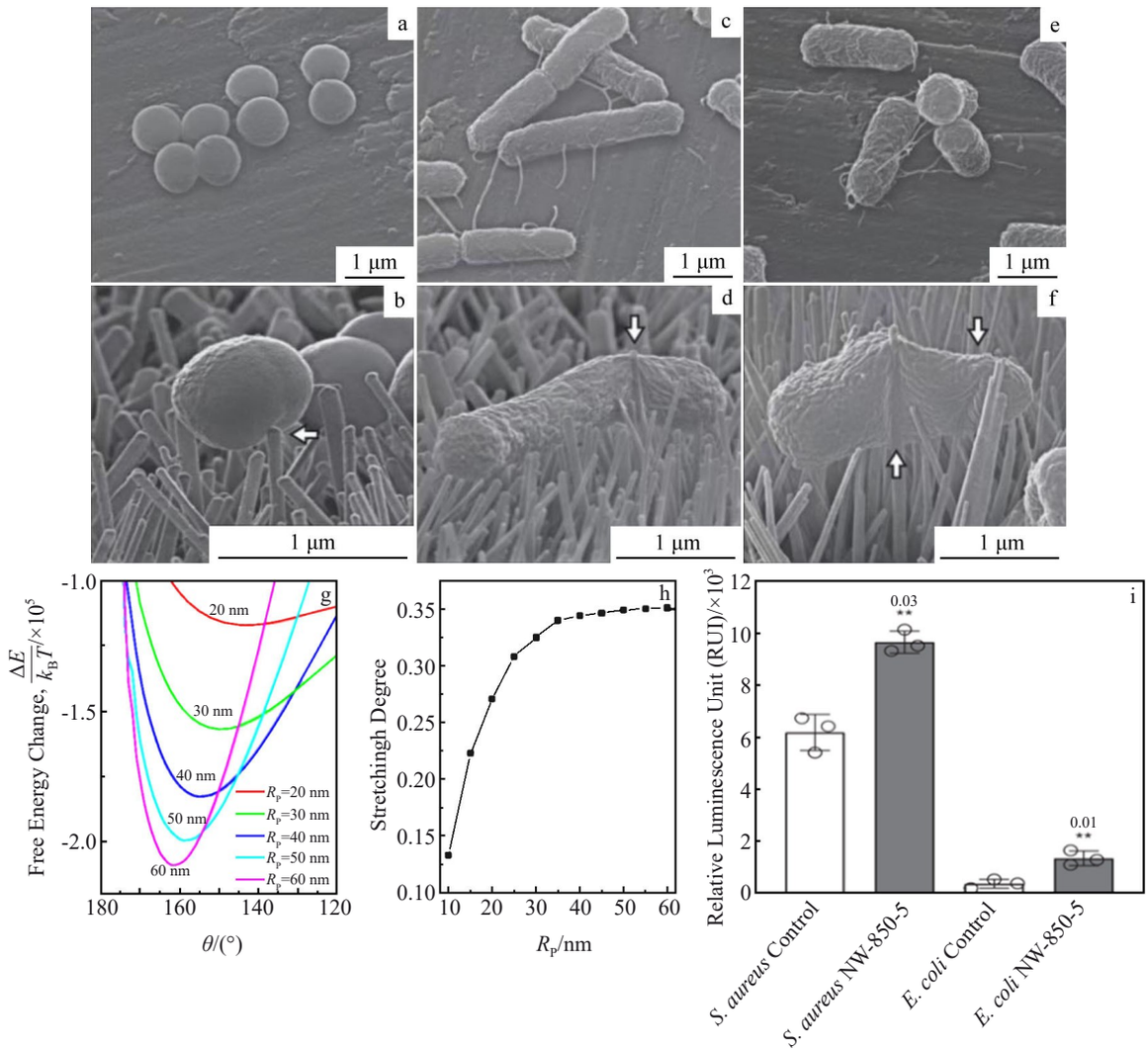

Fig.3 SEM images of *S. aureus* (a–b), *E. coli* (c–d), and *K. pneumoniae* (e–f) cultured for 3 h on flat Ti alloy (control) and nanopillar surfaces[31]; relationship between the minima of free energy change and spacing of nanopillars with different radii (R_p) (g); calculated degree of membrane stretching at equilibrium for bacterial cells exposed to nanopillars with varying radii (h)[34]; levels of H_2O_2 in *S. aureus* or *E. coli* after 24 h of incubation on the control or nanopillar surfaces (** indicates statistically significant difference relative to the control) (i)[31]

nanostructures with larger radii increase the induced tension on bacterial membranes, leading to greater membrane stretching and ultimately causing rupture[34, 50]. The maximum spacing between nanopillars should be less than the diameter of the bacteria; otherwise, the bacteria may fall between the nanopillars, preventing bacterial eradication. In addition, larger spacings can induce cytotoxicity in human cells adhering to the implant, rendering it unsuitable for use[52]. Appropriately small spacing can enhance bactericidal effects. Increasing the slope of the structure also enhances its bactericidal effectiveness by increasing the tangential force exerted on bacteria along the sides of the nanopillars[53]. Bacterial cells undergo more pronounced mechanical deformation when in contact with high aspect ratio nanopillars, leading to increased susceptibility of the bacterial membrane to rupture due to stretching[54].

However, according to the report by Jenkins et al[31], the cell-killing ability of biomimetic nanopillars is not only attributed to the nanomechanical stress, but nanostructured surfaces also alter the genomic and proteomic characteristics of bacteria. Nanopillars induce bacterial cell impedance, significantly reducing the ability of bacteria to replicate on the nanopillar surface. Additionally, nanopillars can induce oxidative stress upon contact with bacterial cells, which is effective against both Gram-positive and Gram-negative bacteria (Fig. 3i). These internal chemical changes in bacteria may cumulatively impair processes such as bacterial growth and biofilm formation. It is also indicated that biomimetic nanostructures may possess multiple mechanisms for bacterial killing and offer the potential for targeting various bacterial species. Simultaneously, this reflects the ambiguity and uncertainty in studying bactericidal mechanisms. Although engineering research methods have a long-standing history in these studies, microbiological research has not been fully

explored. Consequently, most researchers focus on observing bacterial penetration and deformation rather than exploring the cellular mechanisms of interactions between bacterial and nanostructured surfaces. Investigating these interactions from an engineering perspective is challenging due to the difficulty in accurately experimentally evaluating and decoupling the influences of geometric, electrical, and interfacial physical factors[51].

2.3 Titania nanotubes

Electrochemical deposition, hydro/solvothermal methods, sol-gel techniques, and atomic layer deposition (ALD), have been utilized to fabricate titania nanotubes (TNTs) and to control their aspect ratio, length, inner and outer diameters, inter-tube spacing, and degree of order[55]. However, achieving controlled growth of TNTs on implants by the aforementioned techniques is significantly limited due to the complex geometry of the implants, expensive equipment or extensive training, and the constraints of cost, time efficiency, or high-temperature and high-pressure reaction conditions. In contrast, electrochemical anodized TNTs exhibit highly ordered structures and extensive specific surface areas, demonstrating good mechanical strength, unique electronic properties, high concentration and mobility of long-lived charge carriers, and various quantum confinement effects, alongside favorable economic benefits[56]. Electrochemical anodization involves immersing metal/alloy implants into an electrochemical cell containing electrolyte of water and fluoride, submerging the counter electrode, and applying a specific voltage/current. Under optimized conditions at room temperature, titania-based self-ordered TNTs can be rapidly fabricated by controlling voltage and water content in the organic electrolyte. Additionally, during the anodization process, fluoride ions are incorporated into the anodic nanostructure, enhancing antibacterial properties[57].

The aspect ratio, diameter, and preparation conditions of TNTs significantly influence their antibacterial efficacy. However, the investigation on the antibacterial mechanisms of TNTs remains considerably lacking. A potential mechanism is that increasing aspect ratio of the nanomorphology may enhance the flexibility of the tubes, leading to increased membrane stretching due to the deflection of the tubes during bacterial adsorption[47]. Experimental results have shown that within a specific range (20–140 nm), larger diameters of TNTs result in a stronger bactericidal effect[58–59].

Besides, the antibacterial effects of TNTs are highly dependent on bacterial growth phases. Liu et al[30] investigated the influence of growth phases on the antibacterial mechanisms of TNTs anodized at different voltages using Gram-positive (*S. aureus*) bacteria. Fig. 4a shows the growth curve of *S. aureus*, which is composed of the lag phase (0–4 h), the logarithmic phase (4–11 h), and the stationary phase (after 11 h). The viability of *S. aureus* on the anodized samples at the three phases shows different behavior, as presented in Fig.4b. The samples anodized at 30 (named TNT-30) and 50 V (named TNT-50) exhibit significantly lower bacterial viability than the control groups at the lag phase, and the cell morphologies on CP-Ti (Fig. 4c) and TNT-50 (Fig. 4d) also show significant anti-adhesion and bactericidal effects of TNTs. At the logarithmic phase, the viability of *S. aureus* on TNTs can still be controlled at a considerably low level. While the inhibition of *S. aureus* on TNTs does not seem to be so efficient at the stationary phase. The antibacterial mechanisms at various growth phases are summarized in Fig. 5. Additionally, Ji et al[60] also reported a similar phenomenon for Gram-negative (*E. coli*) bacteria cultured on the surface of TNTs, as presented in Fig.4e–4f.

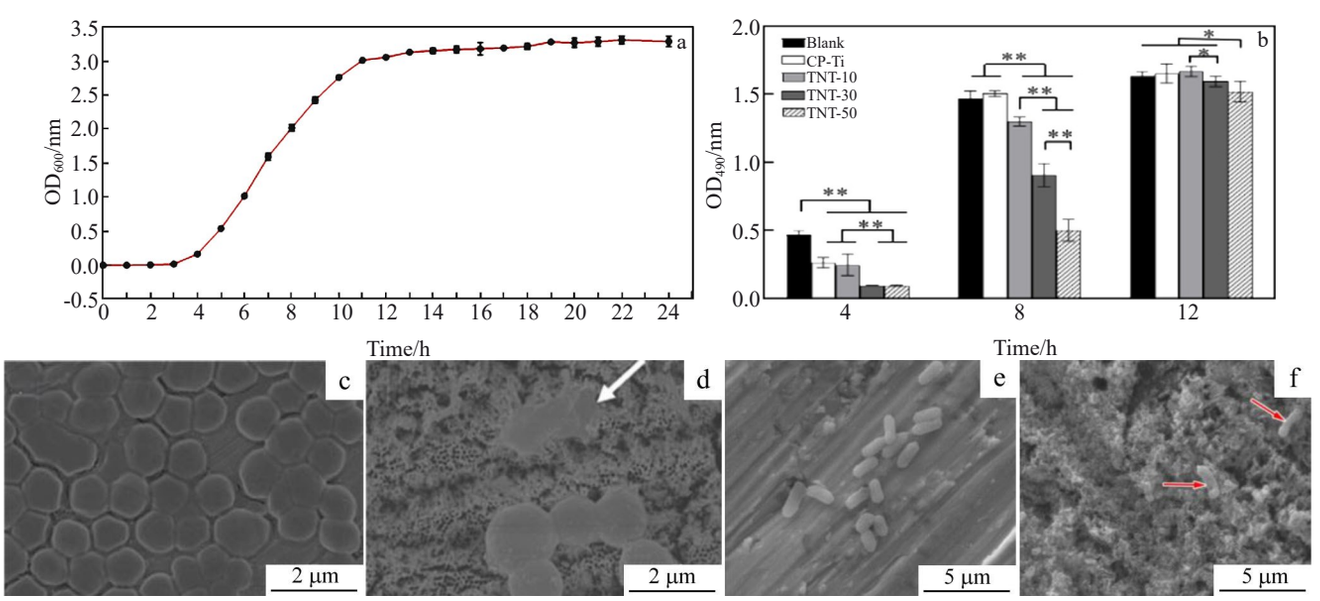

Fig.4 Growth curve of *S. aureus* (a); viability of *S. aureus* cultured for different durations on different samples (* indicates $p < 0.05$; ** indicates $p < 0.01$) (b); morphologies of *S. aureus* (c–d) and *E. coli* (e–f) after incubation for 4 h on CP-Ti (c, e) and TNTs-50 (d, f) samples (white arrow in Fig.4d shows the damaged morphology of *S. aureus*; red arrows in Fig.4f show corrugated or even dead cells)[30, 60]

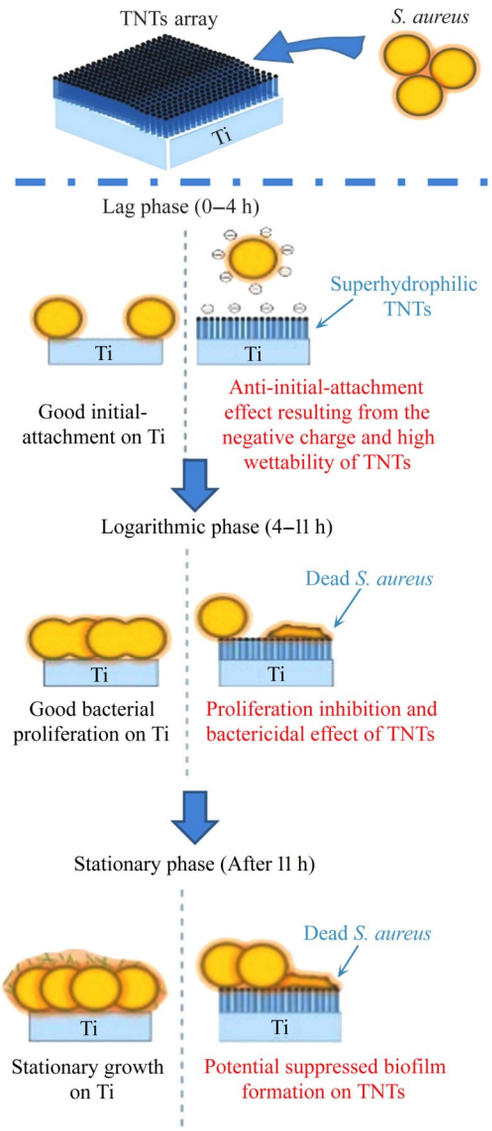

Fig.5 Schematic diagram of dependence of antibacterial behavior of TNTs on growth phase of *S. aureus*[30]

It is important to note that compared with nanopillars, TNTs exhibit higher surface energy, which enhances protein interactions (including adsorption and conformation), thereby improving cell adhesion and tissue growth[57]. Consequently, TNTs show great potential as an ideal Ti-based implant surface, which can both inhibit bacterial behavior and promote osseointegration.

2.4 Other nanostructures

Various methods such as laser treatment, anodic oxidation, and RIE have been applied to fabricate other types of nanostructures on Ti-based implants with antibacterial effects.

Chopra et al[29] fabricated unique nanostructures, including spiny, dagger-like, spiked, and flame-shaped textures, on titanium implants using different anodization parameters (Fig. 6a–6e). These structures differ from conventional TNTs. The anodization of rough substrates leads to uneven distribution of the electric field on the surface protrusions during the anodization process. During the early stages of anodization, the oxide surface exhibits morphological instability, resulting in varying degrees of undulation on the anodic film, which ultimately leads to the self-assembly of anodic structures. The fabricated nanostructures demonstrate strong antibacterial effects, and quantitative analysis revealed that approximately 40% of various bacteria obtained from human saliva on the nanostructured Ti surface were killed within 48 h.

Both RIE[61] and laser treatment[62] can produce microgroove structures (Fig. 6f). The principle of laser treatment involves the formation of periodic grooves on the titanium alloy surface when treated with a low-power laser (4 W for surface treatment). Due to the periodic characteristic of the laser processing, titanium alloy substrate surface exhibits a grooved structure. RIE is based on chemical etching and physical ion bombardment. Ti etching is primarily driven by chemical processes, while TiO_2 etching relies on physical processes. The chemical process is dependent on the reaction between the etching gas and the substrate, whereas the physical process is driven by the kinetic energy of particle beams (i.e., radicals and ion beams) that etch the substrate[63]. Fig. 6g–6h show the microgroove structures on the titanium surface. Microgrooves can trap *P. fluoreescens* and delay direct contact between them, thereby inhibiting biofilm formation[64–65].

3 Hydrophilic and Hydrophobic Antibacterial Properties of Ti Surfaces

The wettability of implant surfaces is determined by their surface chemistry and roughness[66]. Studies show that the water contact angle on rough surfaces is more polarized compared with that on smooth surfaces, i.e., on hydrophobic surfaces, rough surfaces exhibit a larger contact angle, whereas on hydrophilic surfaces, rough surfaces display a smaller contact angle[64]. Protein adhesion and bacterial attachment are influenced by the wettability of the implant surface[29]; for example, hydrophilic surfaces usually effectively enhance protein adsorption[67]; however, the relationship between bacterial adhesion and the hydrophilicity or hydrophobicity of implant surfaces remains controversial. Qi et al[68] developed a model of *E. coli* movement on four hydrophobic surfaces, and demonstrated that more hydrophobic material surfaces exerted a greater surface attraction on *E. coli* during collisions. Boks et al[69] studied the adhesion behavior of four *S. epidermidis* strains on hydrophobic (dimethyldichlorosilane-coated glass) and hydrophilic (glass) substrates. Within 120 s, the adhesion force on hydrophilic glass was significantly stronger than that on hydrophobic coated glass. Due to the gradual formation of hydrogen bonds, the adhesive force was stabilized after approximately 60 s. These cases indicate that bacterial adhesion is influenced by factors beyond wettability, suggesting that wettability may not be the most critical factor[64].

Numerous studies have demonstrated that titanium implant surfaces with superhydrophilic[70] and superhydrophobic[71]

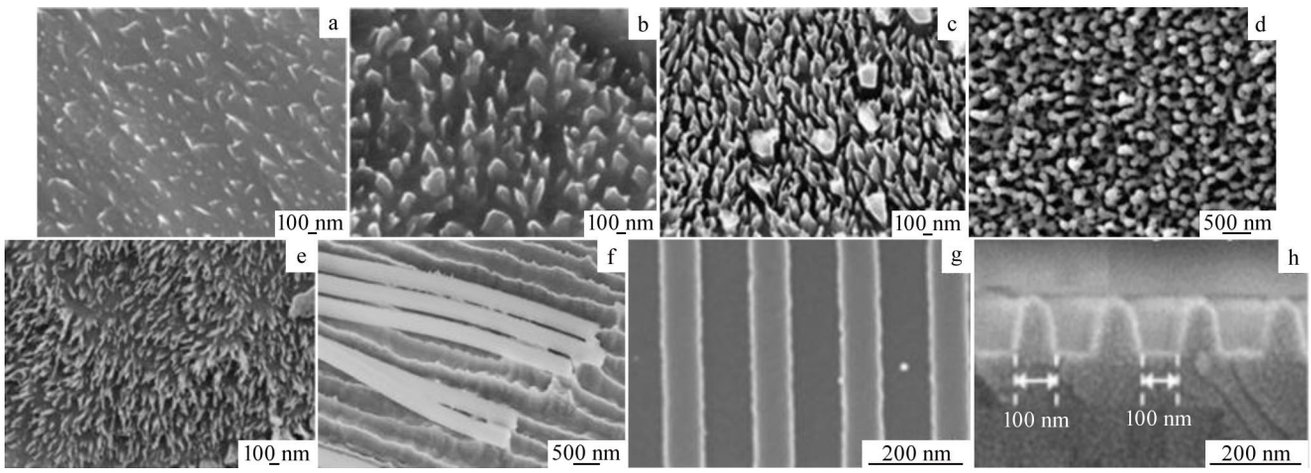

Fig.6 SEM images of Ti-based surfaces with different nanostructures: (a) spinules, (b) daggers, (c) papillae, (d) spikes, and (e) flames[29]; 200 nm linewidth grating (400 nm pitch) (f)[61]; microgroove structures on titanium substrates with a height of 100 nm (g) and 200 nm (h)[43]

properties exhibit significant antibacterial effects. Self-cleaning implant surfaces that display superhydrophobic behavior (water contact angle >150°) exhibit the ability to repel water and oil due to low surface free energy, allowing them to trap air within the liquid[72]. However, the superhydrophobic state is metastable, and the trapped air can eventually be displaced by the liquid[64]. Superhydrophilic surfaces (water contact angle <10°) can also prevent biofilm formation. The reduced bacterial adhesion on superhydrophilic titanium surfaces is attributed to chemical changes that result in decreased carbon content and increased oxygen content on the surface[72].

4 Antibacterial Effects via Physical Stimulus Approaches

Photocatalysis has been widely used for antibacterial applications[20,73]. TiO_2 nanorod arrays have been demonstrated to be highly efficient photosensitizers in antibacterial applications. TiO_2 has a bandgap of 3.2 eV, necessitating activation by ultraviolet (UV) light[74]. Some studies show that enhancing the material's UV light absorption can promote the generation of reactive oxygen species (ROS), which effectively kill bacteria[75–76]. However, UV light is harmful to biological tissues and has poor penetration depth, which is a major obstacle to the widespread use of TiO_2 in antibacterial applications via photocatalysis. Consequently, several modification methods, such as element doping[73,77] and hydrogenation[78], have been employed to reduce the bandgap of TiO_2 and to increase light absorption in the visible and near-infrared regions. Notably, recent research indicates that a bidirectional hydrothermal (aaBH) method can construct periodic titania super-surfaces on Ti alloy implants, enhancing selective near-infrared (NIR, 800 nm) adsorption and effective NIR-activated photocatalytic activity[79]. Compared to element doping and hydrogenation, the super-surface treatment method does not require the introduction of exogenous photosensitizers but rather modulates light behavior through a single nanostructure. Furthermore, the aaBH method is extremely simple and cost-effective, and has significant potential for broader biomedical applications.

The most extensively studied NIR photocatalytic antibacterial mechanisms are primarily categorized into photothermal therapy (PTT) and ROS-related photodynamic therapy (PDT) [80]. PTT generates heat through photothermal conversion, inducing bacterial damage; however, a significant challenge of this therapy is its difficulty in eradicating bacteria at temperatures tolerable to the human body[81]. PDT relies on the ROS produced by materials under light exposure, which leads to the disruption of bacterial cell membranes and protein denaturation. Nevertheless, excessive ROS can induce cytotoxic effects[81]. Both mechanisms are often utilized synergistically to exert antibacterial efficacy within a safe range. As presented in Fig. 7[82], under NIR irradiation, the combined effects of hyperthermia, ROS, and nanomorphology result in outstanding antibacterial and antibiofilm activity. Quantitative detection results showed that the survival rates of *S. aureus* and *E. coli* in the experimental group were approximately 35.8%, demonstrating a strong bactericidal effect[20].

Notably, beyond the photothermal effect, electron transfer under NIR irradiation also exhibits potential antibacterial capabilities. Recently, extracellular electron transfer (EET) between modified surfaces and bacteria has been proposed as a novel tissue-friendly antibacterial strategy[83]. In biological systems, the respiratory processes of bacteria and cells typically involve electron transfer. External electrical signals can disrupt the natural electron transfer process within bacteria, leading to oxidative stress and increased ROS, and ultimately inhibiting bacterial growth[82]. Experimental evidence shows that loading Au[84] or Ag[85] onto TNTs can confer strong antibacterial properties even in the absence of light. When surface-modified Ti implants are in contact with *S. aureus*, EET occurs, wherein electrons are transferred from the bacteria to the implant surface, forming a "bacterial

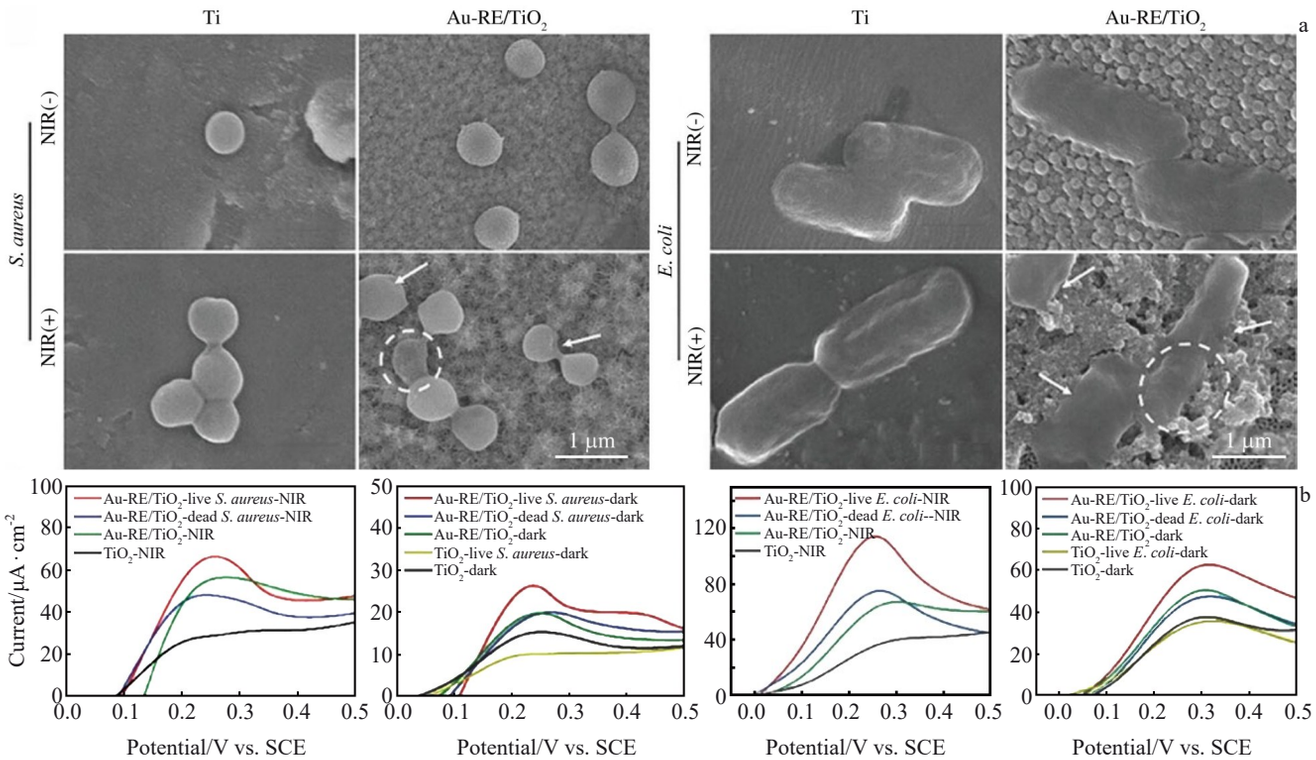

Fig.7 SEM images of *S. aureus* and *E. coli* in different groups (white arrows represent deformation of bacterial cell membrane; white circles indicate bacteria with obvious deformation) (a); current-potential curves of TiO_2 and Au-RE/TiO_2 under dark or 980 nm NIR irradiation conditions (b)[82]

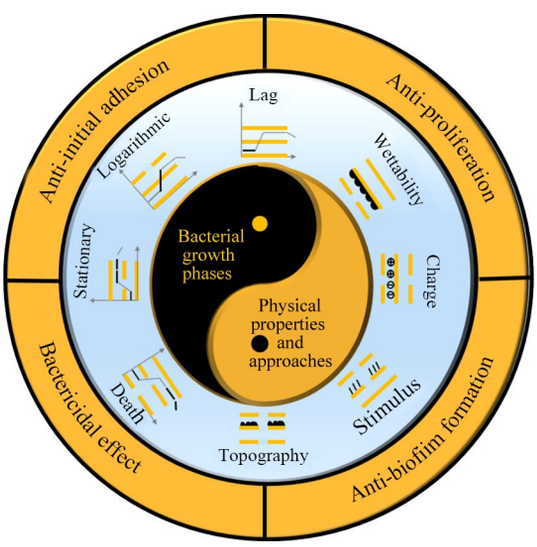

Fig.8 Schematic diagram summarizing the physical antibacterial mechanisms of Ti-based implant surfaces

current" that kills the bacteria. Gold nanoparticles can capture "hot" or "active" electrons from the bacterial respiratory chain and transfer them to TiO_2 via the internal electric field formed by the Schottky barrier, forcing the bacteria to lose electrons. Consequently, the respiratory chain is blocked, triggering a sharp increase in intracellular ROS and leading to bacterial deformation and death[86].

Further experiments revealed that capacitive Ti implants made from carbon-doped TNTs can achieve antibacterial effects upon charging without impairing the growth of osteoblasts. The EET effect is more pronounced on positively charged surfaces than that on neutral ones, likely due to the inherent negative membrane potential of bacteria[87]. Additionally, under NIR light conditions, TNTs enhanced with rare-earth nanoparticles and Au nanoparticles can utilize the up-conversion effect to increase the energy of photoelectrons, thereby enhancing the bactericidal effect of the photo-responsive EET mechanism[82].

5 Summary

1) Physical antibacterial approaches on the surfaces of Ti-based biomaterials are reviewed, and a schematic diagram summarizing the antibacterial mechanisms of these physical approaches is presented in Fig. 8. Generally speaking, the interactions between bacteria and Ti-based implant surfaces are mainly determined by two aspects. On the one hand, the physical properties of implant surfaces as well as physical stimulus approaches, such as the topography (especially the nanomor-phology), wettability, charge, and exogenous light, can tailor the cell fate of bacteria by contact-killing mechanism, anti-protein-adsorption, photocatalysis effect, EET, etc. On the other hand, the antibacterial behavior at different bacterial growth phases (lag phase, logarithmic phase, stationary phase, and death phase) can be categorized

as anti-initial adhesion, anti-proliferation, bactericidal effect, and anti-biofilm formation.

2) Many physical antibacterial surface modifications on Ti-based biomaterials have achieved success in vitro. Nonetheless, most of these strategies have yet to be applied in vivo or even clinically. It can be anticipated that more promising physical antibacterial approaches will be developed and adopted to address Ti-based implant-related infections.

References

1 Abd-Elaziem W, Darwish M A, Hamada A *et al. Materials & Design*[J], 2024, 241: 112850

2 Gan Lu, Yang Bangcheng, Zhang Xingdong. *Rare Metal Materials and Engineering*[J], 2009, 38(7): 1142 (in Chinese)

3 Chen Hong, Ren Yuyu, Ding Jian *et al. Rare Metal Materials and Engineering*[J], 2023, 52(2): 745 (in Chinese)

4 Qiang M, Yang X R, Liu X Y *et al. Rare Metal Materials and Engineering*[J], 2023, 52(5): 1673

5 Okike K, Bhattacharyya T. *JBJS*[J], 2006, 88(12): 2739

6 Tian Tian, Dong Haicheng, Tian Xiaoting *et al. Rare Metal Materials and Engineering*[J], 2016, 45(8): 2098 (in Chinese)

7 Darouiche R O. *New England Journal of Medicine*[J], 2004, 350(14): 1422

8 Campoccia D, Montanaro L, Arciola C R. *Biomaterials*[J], 2006, 27(11): 2331

9 Ni Jiawei, Cao Ziyang, Xu Wei. *Materials China*[J], 2024, 43(6): 525 (in Chinese)

10 Raphel J, Holodniy M, Goodman S B *et al. Biomaterials*[J], 2016, 84: 301

11 Wang Shujun, Gu Xinsheng, Feng Cunao *et al*. *Titanium Industry Progress*[J], 2024, 41(5): 9 (in Chinese)

12 Zhang G, Yang Y, Shi J *et al. Biomaterials*[J], 2021, 269: 120634

13 Chouirfa H, Bouloussa H, Migonney V *et al. Acta Biomaterialia*[J], 2019, 83: 37

14 Darby E M, Trampari E, Siasat P *et al. Nature Reviews Microbiology*[J], 2023, 21(5): 280

15 Kong Wenquan, Wei Kai, Zhao Yao *et al. Rare Metal Materials and Engineering*[J], 2023, 52(7): 2623 (in Chinese)

16 Wu Y, Liao Q, Wu L *et al. Acs Nano*[J], 2021, 15(11): 17854

17 Shi W, Zhao D P, Shang P *et al. Rare Metal Materials and Engineering*[J], 2018, 47(8): 2371

18 Zhang Pudan, Ma Xun, Liu Ping *et al. Rare Metal Materials and Engineering*[J], 2023, 52(12): 4295 (in Chinese)

19 Sanders W E, Sanders C C. *Annual Review of Pharmacology and Toxicology*[J], 1979, 19: 53

20 Zhang X, Zhang G, Chai M *et al. Bioactive Materials*[J], 2021, 6(1): 12

21 Tripathy A, Sen P, Su B *et al. Advances in Colloid and Interface Science*[J], 2017, 248: 85

22 Fadeeva E, Truong V K, Stiesch M *et al. Langmuir*[J], 2011, 27(6): 3012

23 Schaer T P, Stewart S, Hsu B B *et al. Biomaterials*[J], 2012, 33(5): 1245

24 Ma J, Sun Y, Gleichauf K *et al. Langmuir*[J], 2011, 27(16): 10035

25 Bandara C D, Singh S, Afara I O *et al. Acs Applied Materials & Interfaces*[J], 2017, 9(8): 6746

26 Ivanova E P, Hasan J, Webb H K *et al. Small*[J], 2012, 8(16): 2489

27 Cao Y, Su B, Chinnaraj S *et al. Scientific Reports*[J], 2018, 8(1): 1071.

28 Chinnaraj S B, Jayathilake P G, Dawson J *et al. Journal of Materials Science & Technology*[J], 2021, 81: 151

29 Chopra D, Guo T, Jayasree A *et al. Advanced Functional Materials*[J], 2024, 34(30): 2314031

30 Liu P, Zhao Z, Tang J *et al. ACS Biomaterials Science & Engineering*[J], 2022, 8(11): 4976

31 Jenkins J, Mantell J, Neal C *et al. Nature Communications*[J], 2020, 11(1): 1626

32 Pogodin S, Hasan J, Baulin Vladimir A *et al. Biophysical Journal*[J], 2013, 104(4): 835

33 Xue F, Liu J, Guo L *et al. Journal of Theoretical Biology*[J], 2015, 385: 1

34 Li X, Chen T. *Physical Review E*[J], 2016, 93(5): 052419

35 Nowlin K, Boseman A, Covell A *et al. Journal of the Royal Society Interface*[J], 2015, 12(102): 20140999

36 Pier-Francesco A, Adams R J, Waters M G J *et al. Clinical Oral Implants Research*[J], 2006, 17(6): 633

37 Del Curto B, Brunella M F, Giordano C *et al. The International Journal of Artificial Organs*[J], 2005, 28(7): 718

38 Barbour M E, Gandhi N, El-Turki A *et al. Journal of Biomedical Materials Research Part A*[J], 2009, 90a(4): 993

39 Bhadra C M, Khanh Truong V, Pham V T H *et al. Scientific Reports*[J], 2015, 5(1): 16817

40 Bright R, Fernandes D, Wood J *et al. Materials Today Bio*[J], 2022, 13: 100176

41 Diu T, Faruqui N, Sjöström T *et al. Scientific Reports*[J], 2014, 4(1): 7122

42 Ishak M I, Delint R C, Liu X *et al. Biomaterials Advances*[J], 2024, 158: 213766.

43 Shiozawa M, Takeuchi H, Akiba Y *et al. Scientific Reports*[J], 2020, 10(1): 2438

44 Sjöström T, Nobbs A H, Su B. *Materials Letters*[J], 2016, 167: 22

45 Hasan J, Jain S, Chatterjee K. *Scientific Reports*[J], 2017, 7(1): 41118

46 Ebl T D F. *Draw Beam for Electron Beam Lithography Instructions for Use*[M]. Brno: Czech Republic, 2014

47 Linklater D P, Baulin V A, Juodkazis S *et al. Nature Reviews Microbiology*[J], 2021, 19(1): 8

48 Hazell G, Fisher L E, Murray W A *et al. Journal of Colloid and Interface Science*[J], 2018, 528: 389

49 Senevirathne S W M A I, Hasan J, Mathew A *et al. RSC*

Advances[J], 2021, 11(3): 1883
50 Zahir T, Pesek J, Franke S *et al. Microorganisms*[J], 2020, 8(2): 186
51 Hawi S, Goel S, Kumar V *et al. ACS Applied Nano Materials*[J], 2022, 5(1): 1
52 Mirzaali M J, Van Dongen I C P, Tümer N *et al. Nanotechnology*[J], 2018, 29(43): 43lt02
53 Mo S, Mehrjou B, Tang K *et al. Chemical Engineering Journal*[J], 2020, 392: 123736
54 Kelleher S M, Habimana O, Lawler J *et al. ACS Applied Materials & Interfaces*[J], 2016, 8(24): 14966
55 Roy P, Berger S, Schmuki P. *Angewandte Chemie International Edition*[J], 2011, 50(13): 2904
56 Rempel A A, Valeeva A A, Vokhmintsev A S *et al. Russian Chemical Reviews*[J], 2021, 90(11): 1397
57 Puckett S D, Taylor E, Raimondo T *et al. Biomaterials*[J], 2010, 31(4): 706
58 Anitha V C, Lee J H, Lee J *et al. Nanotechnology*[J], 2015, 26(6): 065102
59 Ercan B, Taylor E, Alpaslan E *et al. Nanotechnology*[J], 2011, 22(29): 295102
60 Ji X W, Liu P T, Tang J C *et al. Transactions of Nonferrous Metals Society of China*[J], 2021, 31(12): 3821
61 Woo B W K, Gott S C, Peck R A *et al. ACS Applied Materials & Interfaces*[J], 2017, 9(23): 20161
62 Yang F, Zhang Z, Li Y *et al. ACS Biomaterials Science & Engineering*[J], 2022, 8(6): 2419
63 Ganjian M, Modaresifar K, Zhang H *et al. Scientific Reports*[J], 2019, 9(1): 18815
64 Yang K, Shi J, Wang L *et al. Journal of Materials Science & Technology*[J], 2022, 99: 82
65 Díaz C, Salvarezza R C, Fernández Lorenzo De Mele M A *et al. ACS Applied Materials & Interfaces*[J], 2010, 2(9): 2530
66 Zhao D P, Tang J C, Nie H M *et al. Rare Metals*[J], 2018, 37(12): 1055
67 Kopf B S, Ruch S, Berner S *et al. Journal of Biomedical Materials Research Part A*[J], 2015, 103(8): 2661
68 Qi M, Gong X, Wu B *et al. Langmuir*[J], 2017, 33(14): 3525
69 Boks N P, Busscher H J, Van Der Mei H C *et al. Langmuir*[J], 2008, 24(22): 12990
70 Shibata Y, Suzuki D, Omori S *et al. Biomaterials*[J], 2010, 31(33): 8546
71 Bartlet K, Movafaghi S, Dasi L P *et al. Colloids and Surfaces B: Biointerfaces*[J], 2018, 166: 179
72 Shao H, Ma M, Wang Q *et al. Frontiers In Bioengineering and Biotechnology*[J], 2022, 10: 1000401
73 Su K, Tan L, Liu X *et al. ACS Nano*[J], 2020, 14(2): 2077
74 Miyauchi M, Nakajima A, Watanabe T *et al. Chemistry of Materials*[J], 2002, 14(6): 2812
75 Hatoko M, Komasa S, Zhang H *et al. International Journal of Molecular Sciences*[J], 2019, 20(23): 5991
76 Si Y, Liu H, Yu H *et al. Surface and Coatings Technology*[J], 2022, 431: 128008
77 Kawashita M, Endo N, Watanabe T *et al. Colloids and Surfaces B: Biointerfaces*[J], 2016, 145: 285
78 Echeverrigaray F G, Zanatta A R, Alvarez F. *Journal of Materials Research and Technology*[J], 2021, 12: 1623
79 Yang M, Qiu S, Coy E *et al. Advanced Materials*[J], 2022, 34(6): 2106314
80 Ren Y, Liu H, Liu X *et al. Cell Reports Physical Science*[J], 2020, 1(11): 100245
81 Bai X, Yang Y, Zheng W *et al. Materials Chemistry Frontiers*[J], 2023, 7(3): 355
82 Tang Y, Wang K, Wu B *et al. Advanced Materials*[J], 2024, 36(2): 2307756
83 Wang G, Jin W, Qasim A M *et al. Biomaterials*[J], 2017, 124: 25
84 Li J, Zhou H, Qian S *et al. Applied Physics Letters*[J], 2014, 104(26): 261110
85 Cao H, Qiao Y, Liu X *et al. Acta Biomaterialia*[J], 2013, 9(2): 5100
86 Wang G, Feng H, Gao A *et al. ACS Applied Materials & Interfaces*[J], 2016, 8(37): 24509
87 Wang G, Feng H, Hu L *et al. Nature Communications*[J], 2018, 9(1): 2055

钛基植入材料的物理抗菌表面修饰

张　哲，刘　慧，林漫峰，蔡宗原，赵大鹏
(湖南大学 生物学院，湖南 长沙 410082)

摘　要：钛基植入体的感染是其临床应用的重要挑战，特别是当植入体表面形成了生物膜之后。抗生素、金属纳米颗粒和抗菌肽等抗菌药物已经广泛用于治疗钛植入体的感染。然而，这些化学手段具有潜在的毒性、抗生素抗药性以及长效抗菌效果不足等缺点。因此，钛基植入体的物理抗菌表面正吸引着越来越多的关注。概述了不同的钛基生物材料表面仅依靠植入体本身的物理性质（如纳米拓扑结构）或外源性物理刺激（如光催化）对各种细菌的抗菌效果。影响物理抗菌过程的因素有很多，包括纳米拓扑结构的尺寸、形貌和密度以及细菌生长周期等。此外，对钛基植入材料不同物理抗菌表面的机理进行了总结。

关键词：物理抗菌行为；表面修饰；钛合金；植入体

作者简介：张　哲，男，2001年生，硕士生，湖南大学生物学院，湖南 长沙 410082，E-mail：z1895@hnu.edu.cn